ORIGINAL ARTICLE

Intracerebral Hemorrhage–Induced Brain Injury in Rats: the Role of Extracellular Peroxiredoxin 2

Liheng Bian[1,2] · Jingwei Zhang[1] · Ming Wang[1] · Richard F. Keep[1] · Guohua Xi[1] · Ya Hua[1]

Abstract
Red blood cell (RBC) lysis within the hematoma causes brain injury following intracerebral hemorrhage. Peroxiredoxin 2 (PRX-2) is the third most abundant protein in RBCs and this study examined the potential role of PRX-2 in inducing brain injury in rats. First, adult male Sprague-Dawley rats had an intracaudate injection of lysed RBCs or saline. Brains were harvested at 1 h to measure PRX-2 levels. Second, rats had an intracaudate injection of either recombinant PRX-2, heat-inactivated PRX-2, or saline. Third, rats had intracaudate co-injection of lysed RBCs with conoidin A, a PRX-2 inhibitor, or vehicle. For the second and third parts of studies, behavioral tests were performed and all rats had magnetic resonance imaging prior to euthanasia for brain immunohistochemistry and Western blotting. We found that brain PRX-2 levels were increased after lysed RBC injection. Intracaudate injection of PRX-2 resulted in blood-brain barrier disruption, brain swelling, neutrophil infiltration, microglia activation, neuronal death, and neurological deficits. Intracerebral injection of lysed RBCs induced brain injury, which was reduced by conoidin A. These results suggest that extracellular PRX-2 released from hematoma can cause brain injury following brain hemorrhage and could be a potential therapeutic target.

Keywords Blood-brain barrier · Brain swelling · Intracerebral hemorrhage · Neutrophils · Peroxiredoxin 2

Spontaneous intracerebral hemorrhage (ICH) remains a significant cause of morbidity and mortality worldwide [1]. After the ictus of intracerebral hemorrhage, hemolysis in the hematoma occurs as soon as the first day [2]. Red blood cell (RBC) lysis causes brain edema, neuronal death, and neurological deficits [3] and our prior studies have implicated that hemoglobin and carbonic anhydrase-1 from RBCs are involved in brain damage after ICH [4, 5].

Peroxiredoxin 2 (PRX-2) as well as hemoglobin and carbonic anhydrase-1 are three proteins in the RBC with high concentrations [6]. Intracellular PRX-2 has important anti-oxidant effects in various cell types including RBCs and neurons. However, extracellular PRX-2 can act as an inflammatory mediator as one of the damage-associated molecular patterns (DAMPs), promoting microglia/macrophages to release various pro-inflammatory factors [7–10]. For example, Shichita et al. observed that peroxiredoxins, including PRX-2, released from dead brain cells to extracellular space after brain ischemia could increase inflammatory cytokine expression in macrophages and that antibodies neutralizing extracellular PRXs reduced inflammatory cytokine levels and infarct volume [9]. A recent study found that extracellular PRX-2 in cerebrospinal fluid after subarachnoid hemorrhage causes microglial activation and neuronal apoptosis [11]. However, the role of extracellular PRX-2 after ICH has not been elucidated. The current study, therefore, investigated the following: (1) whether brain PRX-2 levels are increased after intracerebral injection of lysed RBCs; (2) whether intracerebral injection of PRX-2 causes brain injury; and (3) whether conoidin A, an inhibitor of PRX-2, attenuates brain damage caused by lysed RBCs.

Liheng Bian and Jingwei Zhang contributed equally to this work.

✉ Ya Hua
  yahua@umich.edu

1   Department of Neurosurgery, University of Michigan, R5018 BSRB, 109 Zina Pitcher Place, Ann Arbor, MI 48109-2200, USA

2   Department of Neurology, Beijing Tiantan Hospital, Capital Medical University, Beijing, China

Material and Methods

Animal Preparation and Intracerebral Infusion

The protocols for these animal procedures were approved by the University of Michigan Institutional Animal Care and Use Committee. Eighty male adult Sprague-Dawley (SD) rats (260–340 g, Charles River Laboratories, Portage, MI) were used in this study. Rats were anesthetized with pentobarbital (50 mg/kg; i.p.) and body temperature was maintained at 37 °C using a feedback-controlled heating pad. Rats were fixed in a stereotactic frame (David Kopf Instruments, Tujunga, CA). After midline scalp incision, a cranial burr hole (1 mm) was drilled through the skull on the right coronal suture 3.5 mm lateral to the midline. A 26-gauge needle was inserted into the right basal ganglia (coordinates—0.2 mm anterior, 5.5 mm ventral and 3.5 mm lateral to the bregma). Lysed RBCs, saline, heat-inactivated PRX-2 [PRX-2(-)], recombinant PRX-2, lysed RBCs+dimethyl sulfoxide (DMSO), or lysed RBCs+conoidin A (in DMSO) were injected using a microinfusion pump (Harvard Apparatus Inc.) at a rate of 1.5 µl/min. The burr hole was filled with bone wax, and the skin sutured closed. The study complies with the ARRIVE guidelines for reporting in vivo experiments. Randomized was carried out using odd/even numbers.

Conoidin A, a mammalian PRX-2 inhibitor (Cayman, Ann Arbor) was diluted in dimethyl sulfoxide (DMSO). The final concentration co-injected with lysed RBCs was 50 µM.

Experimental Groups

There are four parts in this study. In the first part, rats had an intracerebral injection of lysed RBCs (15 µl, $n = 5$) or saline ($n = 5$, 15 µl) and were euthanized at 1 h after surgery for Western blotting analysis.

In the second part, rats received an intracerebral injection of either recombinant rat PRX-2 (15 µl, 1 mg/ml, Novus biological, NBP2-52150, $n = 13$), PRX-2(-) ($n = 8$), or saline (15 µl, $n = 12$). All rats had T2-weighted magnetic resonance imaging (MRI) and behavioral testing at 24 h. The rats were then euthanized for brain histology ($n = 9$ for PRX-2 group and $n = 8$ for saline group) or Western blots ($n = 4$ for both groups).

In the third part, rats received an intracerebral injection of either recombinant rat PRX-2 (15 µl, 1 mg/ml, $n = 9$) or saline (15 µl, $n = 9$). All rats had T2-weighted magnetic resonance imaging (MRI) and behavioral testing at 24 and 72 h. The rats were then euthanized for brain histology.

In the fourth part, rats had an intracerebral injection of 15 µl either lysed RBCs with vehicle (DMSO; concentration, 1 µl in 100 µl lysed RBC; $n = 9$) or lysed RBC with conoidin A (5 mM in DMSO; 50 µM final concentration in lysed RBCs, $n = 10$). All rats had T2- and T2* weighted MRI, as well as behavioral tests at 24 h. The rats were then euthanized for brain histology.

No rats died in this study. One rat from the PRX-2 group and another from lysed RBCs+conoidin A group were excluded from brain histology measurements because of poor brain perfusion. However, MRI images and behavioral results of the two rats were still used in this study.

MRI and Brain Swelling Measurement

Rats were anesthetized with 2% isoflurance during MRI examination on a 9.4-T MRI scanner (Varian Inc., Palo Alto, CA). The following parameters were chosen: repetition time (TR)/effective echo time (TE), 4000/60 ms for T2 MRI; a field of view (FOV), 35 × 35 mm; matrix, 256 × 256 pixel; slice thickness, 0.5 mm. All MRI images were measured using NIH ImageJ. Brain swelling was calculated on MRI as follows: volume of ([ipsilateral hemisphere−contralateral hemisphere]/volume of contralateral hemisphere) × 100% [12].

Immunohistochemistry

Immunohistochemistry staining was performed as previously described [12, 13]. Rats were anesthetized with pentobarbital (50 mg/kg) and underwent trans-cardiac perfusion with 4% paraformaldehyde. OCT compound embedded brains were sliced into 18 µm sections. The primary antibodies were sheep anti-albumin IgG (Bethyl, A110-134P, 1:1000), rabbit anti-IBA1 IgG (Proteintech, 10904-1-AP, 1:200) and rabbit anti-myeloperoxidase IgG (ThermoFisher, PA5-16672, 1:400). Negative controls omitted the primary antibody.

Fluoro-Jade C Staining

For assessment of neuronal degeneration, rat brain sections were stained with Fluoro-Jade C (Millipore, AG325) [5].

Western Blot Analysis

Western blot analysis was performed as described previously [14]. Rats were anesthetized and brains were perfused with 0.1 mol/l phosphate-buffered saline. Brains were then removed and a 3-mm thick coronal slice was cut centered on the injection site. The slice was separated into the ipsilateral and contralateral basal ganglia. The primary antibodies were rabbit anti-peroxiredoxin 2 (Novus biologicals, NBP2-67887, 1:10,000), sheep anti-albumin (Bethyl, A110-134P, 1:10,000), and mouse anti-β-actin (Sigma-Aldrich, 1:10,000). The secondary antibodies were goat anti-rabbit IgG (Bio-Rad, 1:4000) and goat anti-mouse IgG (Bio-Rad, 1:4000).
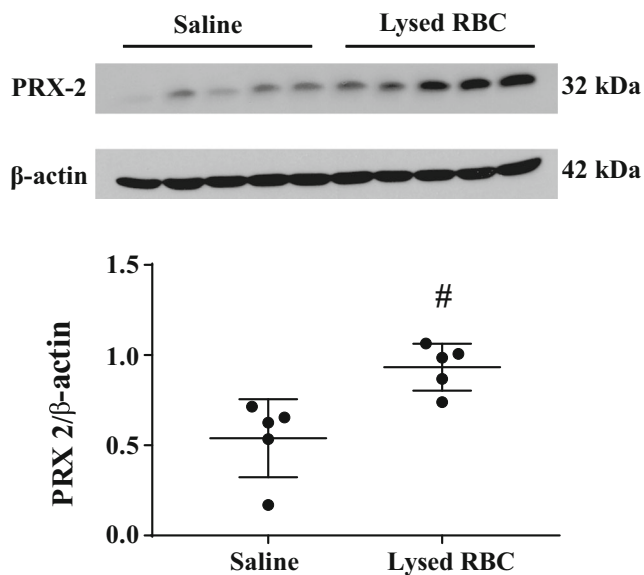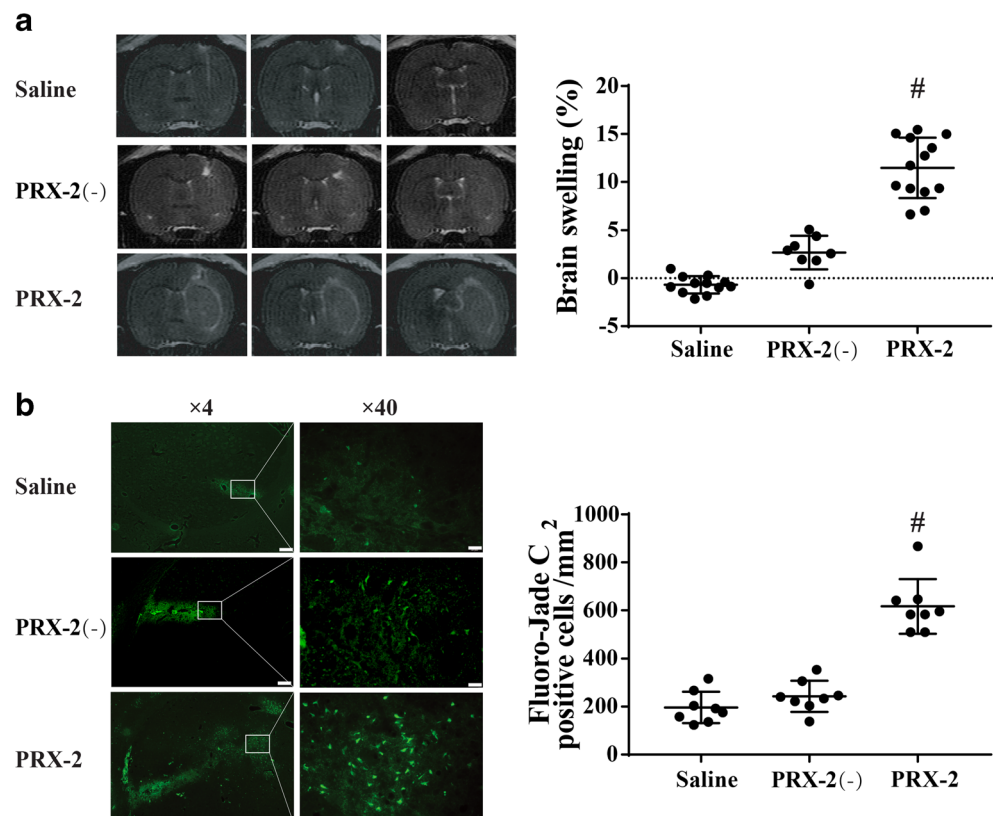
Fig. 1 Western blot assessing PRX-2 levels in the ipsilateral basal ganglia at 1 h after lysed RBCs or saline injection (15 μl). Values are means ± SD; $n = 5$ for both groups; #$P < 0.01$ vs. saline group by the Student t test

Cell Counting

Cell counting was performed on brain coronal sections in a blinded manner. High power images (× 40 magnification) were taken of three brain areas in the ipsilateral caudate. Three slides from each brain with each slide containing three

fields of interest were digitized. All measurements were repeated three times and the mean value was used.

Behavioral Tests

Vibrissae-elicited forelimb placing, forelimb use asymmetry, and corner turn tests were performed for behavioral assessment by a blinded investigator as previously described [15].
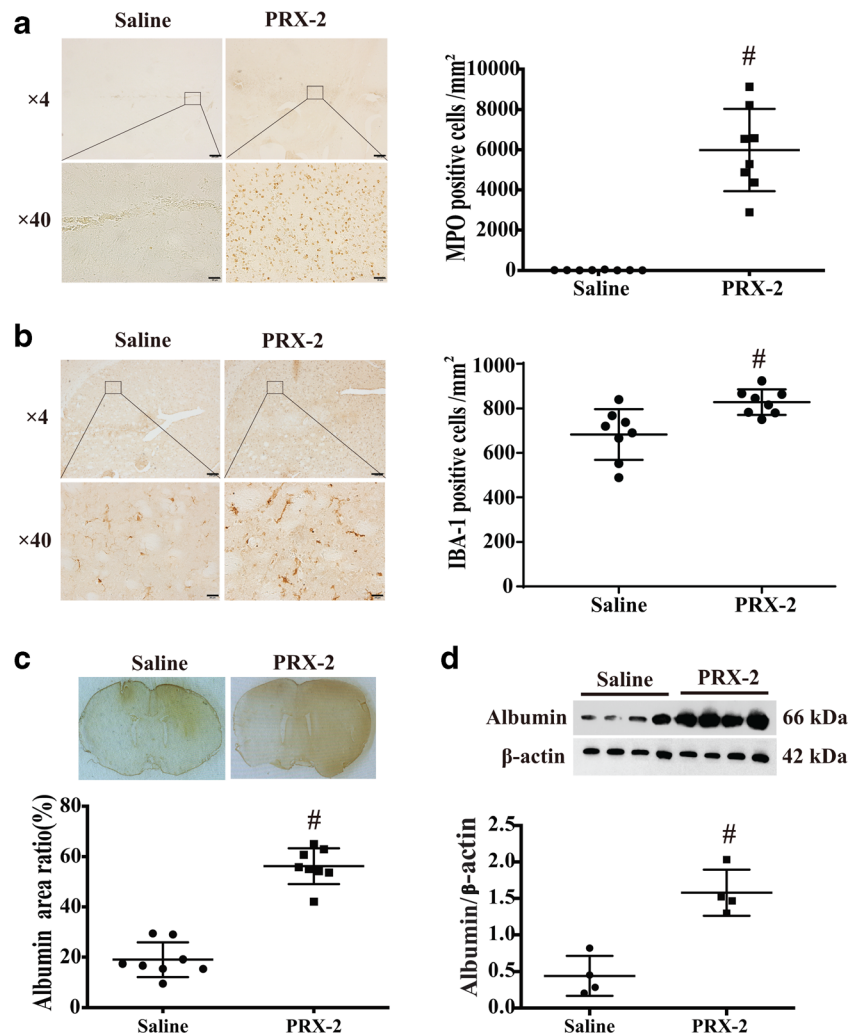
Statistical Analysis

All values are expressed as mean ± SD. Data were analyzed with Student's t test and one-way ANOVA test with the Tukey post hoc test. Significant levels were set at $P < 0.05$.

Results

Injection of Lysed RBCs Increased Brain PRX-2 Protein Levels

PRX-2 protein levels in the ipsilateral basal ganglia were assessed 1 h after injection of 15 μl lysed RBCs or saline injection by Western blotting. Injection of lysed RBCS increased brain PRX-2 levels (PRX-2/β-actin, 0.77 ± 0.12 vs. 0.40 ± 0.17 in saline group; $P < 0.01$, Fig. 1).

Fig. 2 **a** T2 MRI assessment of brain swelling at day 1 after the injection of saline, heat-inactivated PRX-2 (PRX-2(-)) or PRX-2. Values are mean ± SD; $n = 12$ for saline, $n = 8$ for PRX-2(-), $n = 13$ for PRX-2; #$P < 0.01$ vs. saline and PRX-2(-) by one-way ANOVA test with the Tukey post hoc test. **b** Fluoro-Jade C positive cells in the ipsilateral basal ganglia at day 1 after intra-caudate injection of either saline, PRX-2(-) or PRX-2. Values are means ± SD; $n = 8$ for all groups; #$P < 0.01$ vs. saline and PRX-2(-) by one-way ANOVA test with the Tukey post hoc test. Left scale bar = 200 μm; right scale bar = 20 μm

Fig. 3 **a** Myeloperoxidase (MPO) staining in the ipsilateral basal ganglia at day 1 after intracaudate injection of either saline or PRX-2. Values (number of MPO-positive cells/mm²) are means ± SD; $n = 8$ for both groups; $\#P < 0.01$ vs. the saline group by the Student t test. Upper scale bar = 200 μm, lower scale bar = 20 μm. **b** IBA-1 staining in the ipsilateral basal ganglia at day 1 after intracaudate injection of either saline or PRX-2. Values (number of IBA-1 positive cells/mm²) are means ± SD; $n = 8$ for both groups; $\#P < 0.01$ vs. saline group by the Student t test. Upper scale bar = 200 μm, lower scale bar = 20 μm. **c** Albumin immunoreactivity at day 1 after injection. Values (ratio of albumin positive area/whole brain section area) are means ± SD; $n = 8$ for both groups; $\#P < 0.01$ vs. saline group by the Student t test. **d** Albumin protein levels determined by Western blot analysis in the ipsilateral basal ganglia. Values (ratio to β-actin) are means ± SD; $n = 4$ for both groups; $\#P < 0.01$ vs. saline group by the Student t test

Injection of Exogenous PRX-2 Caused Brain Swelling, Neuronal Death, Inflammation, BBB Disruption, and Neurological Deficits

T2-weighted MRI was performed to examine brain swelling at day 1 after 15 μl of recombinant rat PRX-2 injection into the right basal ganglia. PRX-2 injection resulted significant brain swelling in the ipsilateral hemisphere ($11.46 \pm 3.15\%$ increase vs. contralateral) compared with heat-inactivated PRX-2 (PRX-2 (-)) and saline controls ($P < 0.01$; Fig. 2A). In addition, there were more Fluoro-Jade C positive cells in the PRX-2 group compared with controls (617 ± 113 vs. 243 ± 23 in the PRX-2(-) and 197 ± 66 cell/mm² in the saline control, $P < 0.01$; Fig. 2B).

Myeloperoxidase (MPO) was used as a marker of neutrophils and IBA-1 was used to detect microglia/macrophages. PRX-2 injection caused a very marked increase in the number of MPO-positive cells (5988 ± 2052 vs. 19 ± 13 cell/mm² in saline group; $P < 0.01$; Fig. 3A) and IBA-1 positive cells (829 ± 57 vs. 683 ± 114 cell/mm² in saline group; $P < 0.01$, Fig. 3B) in the ipsilateral basal ganglia.

Blood-brain barrier (BBB) leakage at day 1 after PRX-2 injection was assessed by albumin immunohistochemistry. The albumin positive area (% of whole brain area) of PRX-2 group was significantly higher than in the saline group (56 ± 7 vs. $19 \pm 7\%$; $P < 0.01$; Fig. 3C). Similarly, using Western blot, albumin protein levels in ipsilateral basal ganglia of PRX-2
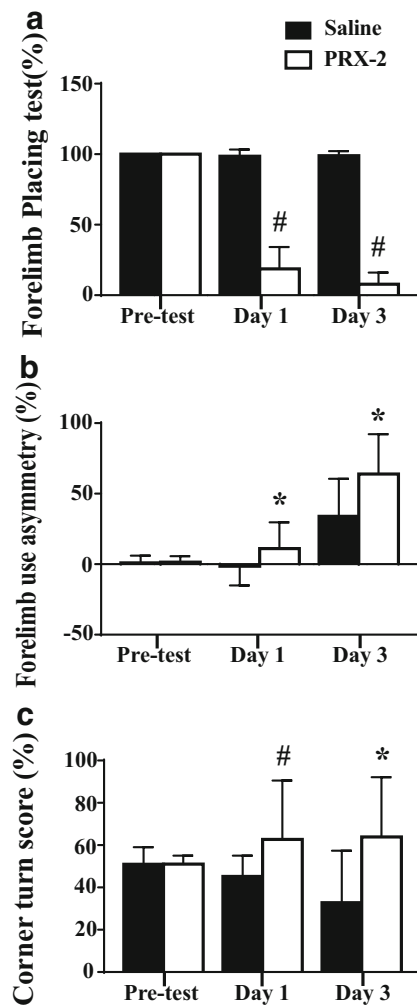
Fig. 4 **a** Forelimb placing, **b** forelimb use asymmetry, and **c** corner turn tests before and after saline or PRX-2 injection. Values are means ± SD; $n = 9$–21 for saline, $n = 9$–22 for PRX-2; #$P < 0.01$ and *$P < 0.05$ vs. saline group at day 1 and day 3 by the Student t test

injected rats were significantly increased compared with saline controls (albumin/β-actin, 1.57 ± 0.32 vs 0.44 ± 0.27; $P < 0.01$, Fig. 3D).

To measure functional outcomes, forelimb placing, forelimb use asymmetry and corner turn tests were undertaken. PRX-2 injected rats had more behavioral deficits than saline-injected rats (forelimb placing, $P < 0.01$, Fig. 4A; forelimb use asymmetry, $P < 0.05$, Fig. 4B; corner turn, day 1, $P < 0.01$ and day 3, $P < 0.05$, Fig. 4C).

Co-injection of Conoidin A Attenuated Lysed RBC-Induced Brain Swelling, Neuronal Death, Neutrophil Infiltration, and Neurological Deficits

Co-injection of a PRX-2 inhibitor, conoidin A resulted in significantly less brain swelling at 24 h compared with co-injection of vehicle. Brain swelling was $2.09 \pm 1.53\%$ in lysed

RBCs + conoidin A vs. $8.52 \pm 2.39\%$ in lysed RBCs + vehicle; $P < 0.01$ (Fig. 5A). Conoidin A co-injection also attenuated lysed RBCs induced neuronal degeneration as assessed by Fluoro-Jade C staining (414 ± 129 vs 760 ± 203 cells/mm^2; $P < 0.01$; Fig. 5B). Using MPO staining for neutrophils [16], there was also significantly less neutrophil infiltration in rats where lysed RBCs were co-injected with conoidin A (644 ± 278 vs. 2724 ± 822 cell/mm^2 with vehicle co-injection, $P < 0.01$; Fig. 5C).

In contrast, conoidin A did not significantly reduce lysed RBC-induced BBB disruption (albumin positive area/whole brain area, $28 \pm 9\%$ vs. $34 \pm 9\%$ in the vehicle group; $P > 0.05$; Fig. 5D). Forelimb placing scores in conoidin A co-injected animals were better than those in the vehicle group ($29.0 \pm 13.7\%$ vs. $3.3 \pm 7.1\%$ in vehicle group; $P < 0.01$; Fig. 6A). However, there were no significant differences between the groups in forelimb use asymmetry ($32.2 \pm 13.7\%$ in conoidin A group vs. $24.8 \pm 16.0\%$ in vehicle group; $P > 0.05$; Fig. 6B) and corner turn ($87 \pm 17\%$ in conoidin A group vs. $92 \pm 12\%$ in vehicle group; $P > 0.05$; Fig. 6C).

Discussion

This study found that (1) brain PRX-2 protein levels are elevated after injection of lysed RBCs to the basal ganglia of rats; (2) intracaudate injection of PRX-2 can induce brain swelling, neuronal degeneration, inflammation, BBB disruption, and neurological deficits; (3) co-injection of conoidin A, a PRX-2 inhibitor, attenuates lysed RBC-induced brain swelling, neuronal death, neutrophil infiltration, and neurological deficits.

Our previous studies have shown that intracerebral injection of lysed RBCs causes marked brain edema formation [4, 17]. Edema formation induced by lysed RBCs seems to be partly mediated by hemoglobin, the most abundant protein in RBCs with injection of hemoglobin injection itself inducing brain edema [4]. Similarly, injection of carbonic anhydrase-1, another protein highly expressed in erythrocytes, induced brain edema, microglia activation and neuronal death after intracerebral injection [5]. However, the potential role of PRX-2, the third most abundant protein in RBC, in ICH-induced brain injury had not been examined. Peroxiredoxins are a ubiquitous family of anti-oxidant enzymes, with six isoforms (PRX 1-6) in humans [18, 19]. PRX-2 is highly abundant in erythrocytes with a concentration of 5.6 mg/ml in RBCs [6, 20]. Within the central nervous system, PRX-2 is mainly distributed intracellularly in neurons where it acts as a hydrogen peroxide and an organic hydroperoxide scavenger

Fig. 5 a T2 MRI assessment of brain swelling at day 1 after lysed RBCs + DMSO (vehicle) or lysed RBCs + conoidin A injection. Values are mean ± SD; $n = 9$ for vehicle, $n = 10$ for conoidin A; $\#P < 0.01$ vs. vehicle by the Student t test. **b** Fluoro-Jade C (F-JC) staining showing degenerative neurons in the ipsilateral basal ganglia at day 1 after the co-injection of either vehicle or conoidin A with lysed RBCs. Values are means ± SD; $n = 9$ for both groups; $\#P < 0.01$ vs. vehicle by the Student t test. Upper scale bar = 200 μm, lower scale bar = 20 μm. **c** MPO staining showing infiltration neutrophils in the ipsilateral basal ganglia at day 1 after intracaudate co-injection of either vehicle or conoidin A with lysed RBCs. Values are means ± SD; $n = 9$ for both groups; $\#P < 0.01$ vs. vehicle by the Student t test. Upper scale bar = 200 μm, lower scale bar = 20 μm
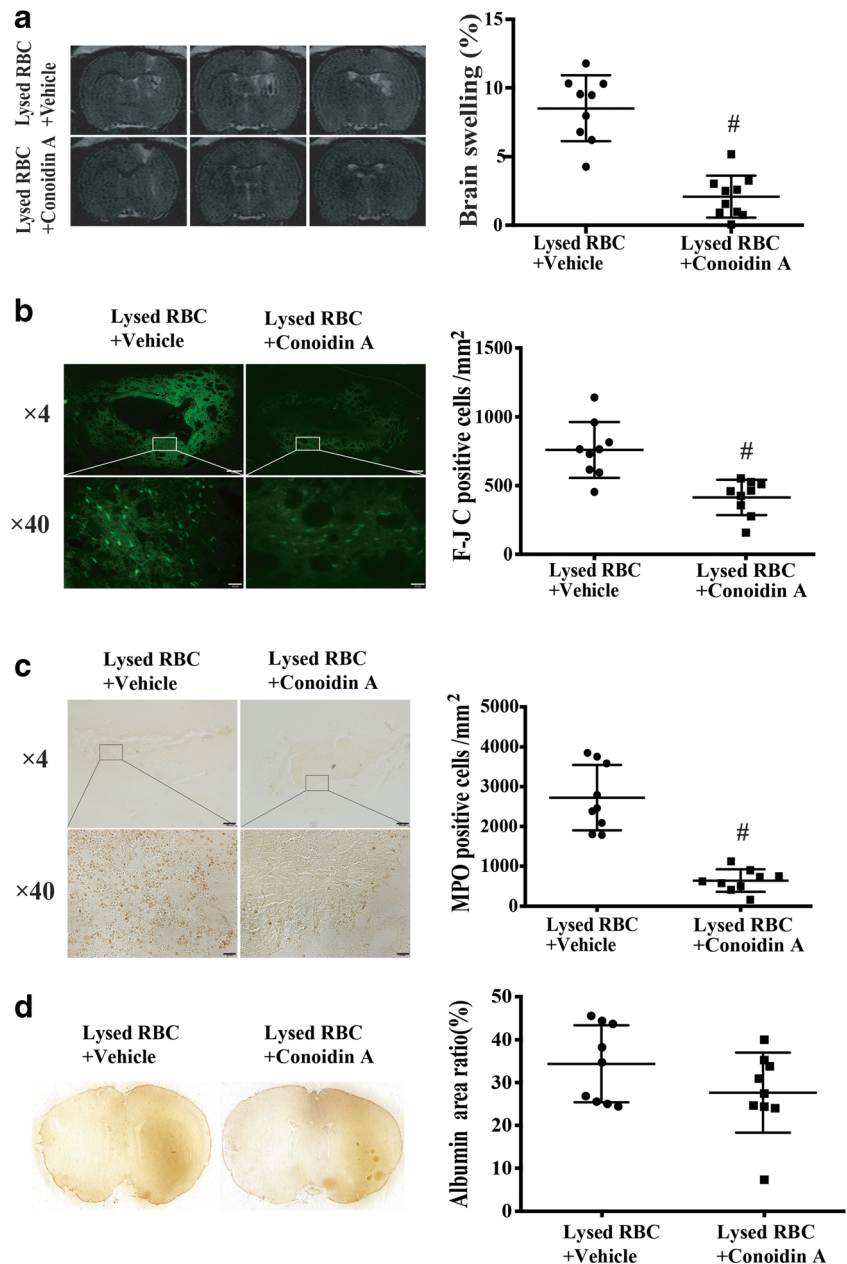
[10, 21]. However, recent studies have indicated that PRX-2 play a detrimental role once released into the extracellular space following stroke. Shichita et al. found that extracellular release of PRX family proteins (PRXs 1, 2, 4-5) from necrotic brain cells contributed to the initiation of post-ischemic inflammation and promoted neuronal death [9]. Furthermore, in a rabbit subarachnoid hemorrhage (SAH) model, higher PRX-2 expression and more neuron deaths were detected in brain cortex when autologous lysed rather than intact erythrocytes were injected into the cistern magna. Although the origin of PRX-2 differs between ischemia and SAH, PRX-2 in both ischemic and hemorrhagic

models accelerated brain injury, indicating its general toxicity irrespective of cellular sources. Consistently, the current study demonstrated that brain PRX-2 levels are increased after lysed RBCs injection into brain parenchyma and administration of exogenous PRX-2 can lead to brain swelling, neuronal degeneration, neutrophil infiltration, blood-brain barrier breakage, and neurological deficits.

The mechanisms underlying PRX-2 induced brain injury are largely unknown. Current data suggest that PRX-2 induces neuroinflammation. As a member of the danger-associated molecular patterns (DAMPs), extracellular PRX-2 can activate microglia/macrophages
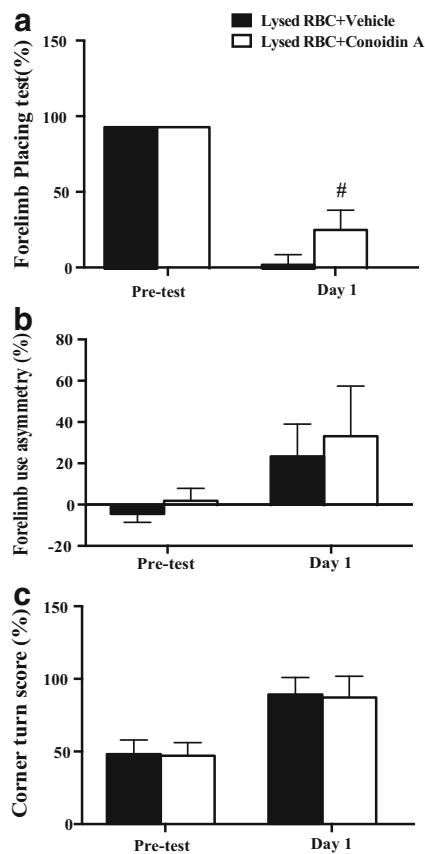
Fig. 6 **a** Forelimb placing, **b** forelimb use asymmetry, and **c** corner turn tests before and 1 day after the intracaudate injection of lysed RBCs + vehicle or lysed RBCs + conoidin A. Values are means ± SD; $n = 9$ for vehicle, $n = 10$ for conoidin A; #$P < 0.01$ vs. vehicle at day 1 by the Student t test

and polymorphonuclear cells which, in turn, produce various pro-inflammatory cytokines and trigger a destructive inflammatory response. In an in vitro study mimicking SAH [10], exogenous PRX-2 were found to interact with toll-like receptor 4 (TLR4) on microglia resulting in microglia activation. In turn, activated microglia upregulate pro-inflammatory factors such as IL-1β, IL-6, and TNF-α, which eventually can cause neuronal apoptosis. Moreover, PRX-2 is constitutively present in macrophages. Macrophage themselves can release PRX-2 facilitating the further production of inflammatory mediators, forming a vicious cycle [7]. In vivo experiments also support an inflammatory injury mechanism. Blocking PRX-2 release [22] or neutralizing extracellular PRX-2[9] attenuate TLR4 signaling activation, reduce inflammatory mediator production and ameliorate neurological deficits after cerebral ischemia. Consistent with these results, marked neutrophil infiltration were observed in the ipsilateral basal ganglia after PRX-2 injection in our study.

The role of extracellular PRX-2 in blood-brain barrier breakdown and neuronal death also deserve further investigation. Plasma levels of PRX-2 are significantly higher in diabetic patients with peripheral atherosclerosis disease than in healthy subjects. This was associated with increased ICAM-1, a biomarker of endothelial dysfunction [23], suggesting a role of circulating PRX-2 in endothelial disruption. However, studies regarding the relationship between extracellular PRX-2 and blood-brain barrier disruption are lacking. PRX-2 administration caused acute neuronal death in our study, suggesting potential direct neuronal toxicity. However, it has been reported that neuronal culture with PRX-2 does not affect neuronal viability in the absence of microglia co-culture [11].

Conoidin A, a specific inhibitor of the PRX family [24], can significantly decrease the oxidized form of PRX-2 by covalently binding to catalytic cysteines [25, 26]. As there is little data of conoidin A use in vivo, we chose a dose (50 μM in lysed RBCs) according to previous in vitro studies [24, 27]. Our current results showed that conoidin A could attenuate the neuronal degeneration, neutrophil infiltration, brain edema and behavioral deficits induced by lysed RBCs, further suggesting a role of PRX 2 in brain tissue damage following ICH. However, conoidin A treatment failed to significantly decrease albumin leakage. BBB disruption after ICH may involve multiple pathways and simply blocking PRX-2 might be not enough [28].

This is a proof-of-concept study to show a role of PRX-2 in brain damage after ICH. There are several limitations in this study: (1) only one dose of PRX-2 and its inhibitor were tested; (2) the effects of PRX-2 on brain injury were only tested during acute phase after injection. Brain injury at other time points should be tested. In particular, the effect of PRX-2 and its inhibitor on long-term behavioral deficits and brain tissue loss should be examined; (3) lysed RBCs were used in the present study. Following experiments should test the roles of conoidin A after whole blood injection which mimics the natural course of intracerebral hemorrhage; and (4) sex and age differences were not examined in this study.

Conclusions

Brain PRX-2 levels are increased after lysed RBCs injection and intracerebral injection of PRX-2 causes acute brain injury. Inhibiting PRX-2 with conoidin A reduces the brain damage induced by lysed RBCs. These results suggest that PRX-2 may be a potential therapeutic target for intracerebral hemorrhage.

Compliance with Ethical Standards

Conflict of Interests The authors declare that they have no conflict of interests.

Ethical Approval All institutional and national guidelines for the care and use of laboratory animals were followed.

References

1. Hemphill JC 3rd, Greenberg SM, Anderson CS, Becker K, Bendok BR, Cushman M, et al. Guidelines for the management of spontaneous intracerebral hemorrhage: a guideline for healthcare professionals from the American Heart Association/American Stroke Association. Stroke. 2015;46:2032–60.

2. Dang G, Yang Y, Wu G, Hua Y, Keep RF, Xi G. Early erythrolysis in the hematoma after experimental intracerebral hemorrhage. Transl Stroke Res. 2017;8:174–82.

3. Xi G, Keep RF, Hoff JT. Mechanisms of brain injury after intracerebral haemorrhage. Lancet Neurol. 2006;5:53–63.

4. Huang FP, Xi G, Keep RF, Hua Y, Nemoianu A, Hoff JT. Brain edema after experimental intracerebral hemorrhage: role of hemoglobin degradation products. J Neurosurg. 2002;96:287–93.

5. Guo F, Hua Y, Wang J, Keep RF, Xi G. Inhibition of carbonic anhydrase reduces brain injury after intracerebral hemorrhage. Transl Stroke Res. 2012;3:130–7.

6. Low FM, Hampton MB, Winterbourn CC. Peroxiredoxin 2 and peroxide metabolism in the erythrocyte. Antioxid Redox Signal. 2008;10:1621–30.

7. Salzano S, Checconi P, Hanschmann EM, Lillig CH, Bowler LD, Chan P, et al. Linkage of inflammation and oxidative stress via release of glutathionylated peroxiredoxin-2, which acts as a danger signal. Proc Natl Acad Sci U S A. 2014;111:12157–62.

8. Garcia-Bonilla L, Iadecola C. Peroxiredoxin sets the brain on fire after stroke. Nat Med. 2012;18:858–9.

9. Shichita T, Hasegawa E, Kimura A, Morita R, Sakaguchi R, Takada I, et al. Peroxiredoxin family proteins are key initiators of post-ischemic inflammation in the brain. Nat Med. 2012;18:911–7.

10. Lu Y, Zhang XS, Zhou XM, Gao YY, Chen CL, Liu JP, et al. Peroxiredoxin 1/2 protects brain against h2o2-induced apoptosis after subarachnoid hemorrhage. FASEB J. 2019; 33:3051–3062.

11. Lu Y, Zhang XS, Zhang ZH, Zhou XM, Gao YY, Liu GJ, et al. Peroxiredoxin 2 activates microglia by interacting with toll-like receptor 4 after subarachnoid hemorrhage. J Neuroinflammation. 2018;15:87.

12. Ni W, Mao S, Xi G, Keep RF, Hua Y. Role of erythrocyte cd47 in intracerebral hematoma clearance. Stroke. 2016;47:505–11.

13. Liu H, Hua Y, Keep RF, Xi G. Brain ceruloplasmin expression after experimental intracerebral hemorrhage and protection against iron-induced brain injury. Transl Stroke Res. 2019;10:112–9.

14. Jin H, Xi G, Keep RF, Wu J, Hua Y. Darpp-32 to quantify intracerebral hemorrhage-induced neuronal death in basal ganglia. Transl Stroke Res. 2013;4:130–4.

15. Hua Y, Schallert T, Keep RF, Wu J, Hoff JT, Xi G. Behavioral tests after intracerebral hemorrhage in the rat. Stroke. 2002;33:2478–84.

16. Gong C, Hoff JT, Keep RF. Acute inflammatory reaction following experimental intracerebral hemorrhage in rat. Brain Res. 2000;871:57–65.

17. Xi G, Keep RF, Hoff JT. Erythrocytes and delayed brain edema formation following intracerebral hemorrhage in rats. J Neurosurg. 1998;89:991–6.

18. Trujillo M, Ferrer-Sueta G, Thomson L, Flohe L, Radi R. Kinetics of peroxiredoxins and their role in the decomposition of peroxynitrite. Subcell Biochem. 2007;44:83–113.

19. Rhee SG, Kang SW, Chang TS, Jeong W, Kim K. Peroxiredoxin, a novel family of peroxidases. IUBMB Life. 2001;52:35–41.

20. Moore RB, Mankad MV, Shriver SK, Mankad VN, Plishker GA. Reconstitution of Ca(2+)-dependent K+ transport in erythrocyte membrane vesicles requires a cytoplasmic protein. J Biol Chem. 1991;266:18964–8.

21. Jin MH, Lee YH, Kim JM, Sun HN, Moon EY, Shong MH, et al. Characterization of neural cell types expressing peroxiredoxins in mouse brain. Neurosci Lett. 2005;381:252–7.

22. Mao XN, Zhou HJ, Yang XJ, Zhao LX, Kuang X, Chen C, et al. Neuroprotective effect of a novel gastrodin derivative against ischemic brain injury: involvement of peroxiredoxin and tlr4 signaling inhibition. Oncotarget. 2017;8:90979–95.

23. El Eter E, Al Masri A, Habib S, Al Zamil H, Al Hersi A, Al Hussein F, et al. Novel links among peroxiredoxins, endothelial dysfunction, and severity of atherosclerosis in type 2 diabetic patients with peripheral atherosclerotic disease. Cell Stress Chaperones. 2014;19:173–81.

24. Ryu DY, Kim KU, Kwon WS, Rahman MS, Khatun A, Pang MG. Peroxiredoxin activity is a major landmark of male fertility. Sci Rep. 2017;7:17174.

25. Haraldsen JD, Liu G, Botting CH, Walton JG, Storm J, Phalen TJ, et al. Identification of conoidin a as a covalent inhibitor of peroxiredoxin ii. Org Biomol Chem. 2009;7:3040–8.

26. Liu G, Botting CH, Evans KM, Walton JA, Xu G, Slawin AM, et al. Optimisation of conoidin a, a peroxiredoxin inhibitor. ChemMedChem. 2010;5:41–5.

27. Nguyen JB, Pool CD, Wong CY, Treger RS, Williams DL, Cappello M, et al. Peroxiredoxin-1 from the human hookworm ancylostoma ceylanicum forms a stable oxidized decamer and is covalently inhibited by conoidin a. Chem Biol. 2013;20:991–1001.

28. Keep RF, Andjelkovic AV, Xiang J, Stamatovic SM, Antonetti DA, Hua Y, et al. Brain endothelial cell junctions after cerebral hemorrhage: changes, mechanisms and therapeutic targets. J Cereb Blood Flow Metab. 2018;38:1255–75.

Publisher's Note Springer Nature remains neutral with regard to jurisdictional claims in published maps and institutional affiliations.